Low-complexity Linear Equalization for 2×2 MIMO-OTFS Signals

G. D. Surabhi and A. Chockalingam
Department of ECE, Indian Institute of Science, Bangalore 560012

***Abstract*—Orthogonal time frequency space (OTFS) modulation is a two-dimensional modulation scheme which has superior performance compared to conventional multicarrier modulation schemes. In this paper, we propose low-complexity linear equalizers for a 2×2 multiple-input-multiple-output (MIMO) OTFS system. The proposed equalizers are designed by exploiting the structure of the effective delay-Doppler MIMO channel matrix in a MIMO-OTFS system. The channel matrix in a MIMO-OTFS system is a block matrix composed of blocks which have a block circulant with circulant block structure. The proposed approach makes use of the properties of block matrices and block circulant matrices to reduce the computational complexity of linear equalizers. For a 2×2 MIMO-OTFS system that uses $N \times M$ OTFS modulation, where N and M denote the number of Doppler and delay bins, respectively, the proposed linear equalizers provide exact solution with a computational complexity of $\mathcal{O}(MN \log MN)$, whereas conventional linear equalizers require a complexity of $\mathcal{O}(M^3N^3)$.**

keywords: *OTFS modulation, MIMO-OTFS, linear equalizers, block circulant matrices, computational complexity.*

I. Introduction

Orthogonal time frequency space (OTFS) modulation is a new waveform design that is well suited to combat the effects of time and frequency selective nature of wireless channels. This modulation scheme was introduced in [1],[2], where it was shown to achieve superior error performance compared to conventional multicarrier modulation schemes like orthogonal frequency division multiplexing (OFDM) in high mobility environments. Fundamentally, OTFS modulation differs from conventional multicarrier modulation schemes in the way it multiplexes information symbols. In OTFS, information symbols are multiplexed in the delay-Doppler domain, unlike in conventional multicarrier modulation techniques where information symbols are multiplexed in the time-frequency domain. The symbols multiplexed in the delay-Doppler domain undergo two-dimensional (2D) periodic convolution with the channel response in the delay-Doppler domain such that each symbol experiences a near-constant channel gain even in rapidly time varying wireless channels [2]-[4]. Further, the channel when represented in the delay-Doppler domain is sparse in nature and exhibits slow variation compared to that in time-frequency representation, thereby reducing the complexity of channel estimation in high Doppler environments.

Detection of OTFS modulated signals has been addressed in several papers in the literature [4]-[9]. OTFS signal detection based on message passing and Markov chain Monte Carlo (MCMC) techniques have been proposed in [4] and [5], respectively. In [6], OTFS has been viewed in the generalized frequency division multiplexing (GFDM) framework and detection is carried out using minimum mean squared error (MMSE) detector. Further, [7] proposes MMSE detection in time-frequency domain which is followed by a non-linear equalizer based on interference cancellation. Low-complexity linear equalization in delay-Doppler domain, exploiting the block circulant nature of the effective delay-Doppler channel in OTFS, has been reported in [8],[9]. While the approach in [8] uses LU decomposition for the design of linear equalizers with reduced complexity, [9] uses eigen value decomposition (EVD) and fast Fourier transforms (FFT) to achieve complexity reduction. The detection techniques mentioned above are proposed for OTFS in a single-input single-output (SISO) setting. The system model and a message passing based signal detection technique for OTFS in a MIMO setting have been presented in [10]. The design and performance of linear equalizers with reduced complexity for OTFS in MIMO setting have not been reported so far in the literature. In this paper, we propose low-complexity zero forcing (ZF) and MMSE equalizers which exploit the inherent structure in the delay-Doppler MIMO channel matrix in a MIMO-OTFS system and achieve significant reduction in computational complexity compared to that of conventional linear equalizers.

The conventional MMSE and ZF equalizers involve inversion of matrices for computing the solutions. The computational complexity required to perform matrix inversion is very high, especially when the dimensions of matrices involved are large. In this paper, we propose an approach that makes use of the structure in the effective delay-Doppler MIMO channel matrix to achieve significant reduction in the computational complexity compared to those of conventional linear equalizers. Specifically, the channel matrix of a MIMO-OTFS system is composed of blocks which have a block circulant with circulant block structure. The proposed approach recognizes this structure and uses it in a 2×2 MIMO-OTFS system to achieve exact MMSE/ZF solution at a significantly reduced order of complexity. For example, the proposed equalizers provide the exact MMSE/ZF solutions at a computational complexity of $\mathcal{O}(MN \log MN)$, whereas conventional linear equalizers require a complexity of $\mathcal{O}(M^3N^3)$.

II. MIMO-OTFS system model

The transforms involved in the transmit and receive sides of OTFS system are presented below.

A. Transforms involved in OTFS modulation

- *Inverse symplectic finite Fourier transform (ISFFT):* MN information symbols are multiplexed on a delay-Doppler grid of size $N \times M$. These symbols in the delay-Doppler

This work was supported in part by the J. C. Bose National Fellowship, Department of Science and Technology, Government of India, Tata Elxsi Limited, Bengaluru 560048, and the Intel India Faculty Excellence Program.

978-1-7281-5478-7/20/$31.00 ©2020 IEEE

domain, denoted by $x[k,l]$, $k = 0,\cdots,N-1$, $l = 0,\cdots,M-1$, $x[k,l] \in \mathbb{A}$, where $\mathbb{A}$ is a conventional modulation alphabet (e.g., QAM), are transmitted in a packet of duration NT in a given bandwidth $B = M\Delta f$, where $\Delta f = \frac{1}{T}$. The symbols $x[k,l]$s in the delay-Doppler domain are first mapped to the time-frequency (TF) plane using ISFFT, as

$$X[n,m] = \frac{1}{MN}\sum_{k=0}^{N-1}\sum_{l=0}^{M-1} x[k,l]e^{j2\pi(\frac{nk}{N}-\frac{ml}{M})}. \quad (1)$$

- *Heisenberg transform:* The TF signal $X[n,m]$ is then converted to time domain for transmission using Heisenberg transform, as

$$x(t) = \sum_{n=0}^{N-1}\sum_{m=0}^{M-1} X[n,m]g_{tx}(t-nT)e^{j2\pi m\Delta f(t-nT)}, \quad (2)$$

  where $g_{tx}(t)$ is the transmit pulse shape.
- *Transmission through the channel:* The time domain signal $x(t)$ is transmitted through the time varying channel, whose complex baseband delay-Doppler channel response is denoted by $h(\tau,\nu)$, where τ and ν denote the delay and Doppler, respectively. The received time domain signal is given by

$$y(t) = \int_\nu\int_\tau h(\tau,\nu)x(t-\tau)e^{j2\pi\nu(t-\tau)}\mathrm{d}\tau\mathrm{d}\nu. \quad (3)$$

- *Wigner transform:* The received signal $y(t)$ is converted into a time-frequency signal using Wigner transform, as

$$Y[n,m] = A_{g_{rx},y}(t,f)|_{t=nT,f=m\Delta f},$$
$$A_{g_{rx},y}(t,f) = \int y(t)g^*_{rx}(t'-t)e^{-j2\pi f(t'-t)}\mathrm{d}t', \quad (4)$$

  where $g_{rx}(t)$ denotes the receive pulse shape.
- *Symplectic finite Fourier transform (SFFT):* Finally, the TF signal $Y[n,m]$ is transformed back to the delay-Doppler domain using SFFT, as

$$y[k,l] = \sum_{n=0}^{N-1}\sum_{m=0}^{M-1} Y[n,m]e^{-j2\pi(\frac{nk}{N}-\frac{ml}{M})}. \quad (5)$$

B. Vectorized input-output (I/O) relation

Using (1)-(5), end-to-end I/O relation can be derived as [3]

$$y[k,l] = \frac{1}{MN}\sum_{l'=0}^{M-1}\sum_{k'=0}^{N-1} x[k',l']h_w\left(\frac{k-k'}{NT},\frac{l-l'}{M\Delta f}\right) + v[k,l], \quad (6)$$

where $h_w\left(\frac{k-k'}{NT},\frac{l-l'}{M\Delta f}\right) = h_w(\nu,\tau)|_{\nu=\frac{k-k'}{NT},\tau=\frac{l-l'}{M\Delta f}}$ and $h_w(\nu,\tau)$ is as defined in [3]. This equation can be vectorized as [4]

$$\mathbf{y} = \mathbf{H}\mathbf{x} + \mathbf{n}, \quad (7)$$

where $\mathbf{x} \in \mathbb{C}^{MN\times 1}$ is the transmitted OTFS vector, $\mathbf{y} \in \mathbb{C}^{MN\times 1}$ is the received OTFS vector, $\mathbf{H} \in \mathbb{C}^{MN\times MN}$ is the effective channel matrix in the delay-Doppler domain, and $\mathbf{n} \in \mathbb{C}^{MN\times 1}$ denotes the noise vector with its entries distributed $\mathcal{CN}(0,\sigma^2)$.

C. OTFS in MIMO setting

Consider a MIMO-OTFS system with n_t transmit and n_r receive antennas. Each transmit antenna transmits an $NM\times 1$ OTFS signal vector. Let $\mathbf{x}_k$ denote the transmit vector from kth transmit antenna and $\mathbf{H}_{lk}$ denote the effective delay-Doppler channel between kth transmit and lth receive antennas. The vectorized I/O relation in MIMO-OTFS is given by [10]

$$\begin{bmatrix}\mathbf{y}_1\\ \mathbf{y}_2\\ \vdots\\ \mathbf{y}_{n_r}\end{bmatrix} = \begin{bmatrix}\mathbf{H}_{11} & \mathbf{H}_{12}\cdots\mathbf{H}_{1n_t}\\ \mathbf{H}_{21} & \mathbf{H}_{22}\cdots\mathbf{N}_{2n_t}\\ \vdots & \\ \mathbf{H}_{n_r1} & \mathbf{H}_{n_r2}\cdots\mathbf{H}_{n_rn_t}\end{bmatrix}\begin{bmatrix}\mathbf{x}_1\\ \mathbf{x}_2\\ \vdots\\ \mathbf{x}_{n_t}\end{bmatrix} + \begin{bmatrix}\mathbf{n}_1\\ \mathbf{n}_2\\ \vdots\\ \mathbf{n}_{n_r}\end{bmatrix}, \quad (8)$$

where $\mathbf{y}_l$ and $\mathbf{n}_l$ denote the received vector and noise vector, respectively, at the lth receive antenna. The vectorized input-output relation in (8) can be compactly written as

$$\mathbf{y}_{\text{MIMO}} = \mathbf{H}_{\text{MIMO}}\mathbf{x}_{\text{MIMO}} + \mathbf{n}_{\text{MIMO}}, \quad (9)$$

where, $\mathbf{y}_{\text{MIMO}} = [\mathbf{y}_1^T\mathbf{y}_2^T\cdots\mathbf{y}_{n_r}^T]^T$, $\mathbf{x}_{\text{MIMO}} = [\mathbf{x}_1^T\mathbf{x}_2^T\cdots\mathbf{x}_{n_t}^T]^T$, and $\mathbf{H}_{\text{MIMO}}$ is the delay-Doppler MIMO channel matrix as described in (8).

III. Low-complexity linear equalizers for 2×2 MIMO-OTFS

Consider a 2×2 MIMO-OTFS system whose vectorized I/O relation can be written in the form (8). The MMSE and ZF solutions are given by $\hat{\mathbf{x}}_{\text{MMSE}} = \mathbf{G}_{\text{MMSE}}\mathbf{y}_{\text{MIMO}}$ and $\hat{\mathbf{x}}_{\text{ZF}} = \mathbf{G}_{\text{ZF}}\mathbf{y}_{\text{MIMO}}$, respectively, where $\mathbf{G}_{\text{MMSE}} = (\mathbf{H}^H_{\text{MIMO}}\mathbf{H}_{\text{MIMO}} + \sigma^2\mathbf{I}_{MNn_r\times MNn_t})^{-1}\mathbf{H}^H_{\text{MIMO}}$ and $\mathbf{G}_{\text{ZF}} = (\mathbf{H}^H_{\text{MIMO}}\mathbf{H}_{\text{MIMO}})^{-1}\mathbf{H}^H_{\text{MIMO}}$. The key idea behind the proposed low-complexity MMSE and ZF equalizers is to compute $\mathbf{G}_{\text{MMSE}}\mathbf{y}_{\text{MIMO}}$ and $\mathbf{G}_{\text{ZF}}\mathbf{y}_{\text{MIMO}}$ with low-complexity using FFTs, IFFTs, and the properties of $\mathbf{H}_{\text{MIMO}}$ and $\mathbf{G}_{\text{MMSE}}$.

A. Low-complexity MMSE equalizer

The effective delay-Doppler MIMO channel matrix in 2×2 MIMO-OTFS systemis a block matrix given by

$$\mathbf{H}_{\text{MIMO}} = \begin{bmatrix}\mathbf{H}_{11} & \mathbf{H}_{12}\\ \mathbf{H}_{21} & \mathbf{H}_{22}\end{bmatrix}. \quad (10)$$

Observe that $\mathbf{H}_{\text{MIMO}}$ in (10) is a block matrix of size $2NM\times 2NM$ with each block $\mathbf{H}_{ij}, i,j \in \{1,2\}$ having a block circulant with circulant block structure. Each of the $\mathbf{H}_{ij}$s in $\mathbf{H}_{\text{MIMO}}$ is a block circulant matrix consisting of M circulant blocks of size $N\times N$. Let $\mathcal{B}_{M,N}$ denote the class of block circulant matrices formed by M circulant blocks of size $N\times N$. Now, $\mathbf{H}_{ij} \in \mathcal{B}_{MN}, i,j \in \{1,2\}$, and hence the matrix $\mathbf{H}_{ij}$ has the eigen value decomposition (EVD) given by [11]

$$\mathbf{H}_{ij} = (\mathbf{F}_M \otimes \mathbf{F}_N)^H\mathbf{\Lambda}_{ij}(\mathbf{F}_M \otimes \mathbf{F}_N), \quad (11)$$

where $\mathbf{F}_M$ and $\mathbf{F}_N$ denote $M\times M$ and $N\times N$, discrete Fourier transform (DFT) matrices respectively, and $\mathbf{\Lambda}_{ij}$ denotes the diagonal matrix which contains the eigen values of $\mathbf{H}_{ij}$. The entries of $\mathbf{\Lambda}_{ij}$ are given by

$$\mathbf{\Lambda}_{ij} = \sum_{k=0}^{M-1}\mathbf{\Omega}_M^k \otimes \mathbf{\Lambda}_{ij}^{(k)}, \quad (12)$$

where $\mathbf{\Omega}_M = \text{diag}\{1,\omega,\cdots,\omega^{M-1}\}$ with $\omega = e^{j2\pi/M}$ and $\mathbf{\Lambda}_{ij}^{(k)}$ denotes the diagonal matrix of size $N\times N$ which contains

the eigen values of kth circulant block of $\mathbf{H}_{ij}$. Now, in order to compute $\mathbf{G}_{\text{MMSE}}\mathbf{y}_{\text{MIMO}}$ and $\mathbf{G}_{\text{ZF}}\mathbf{y}_{\text{MIMO}}$, we make use of some of the properties of $\mathbf{G}_{\text{MMSE}}$ and $\mathbf{G}_{\text{ZF}}$. Towards this, we first prove the following lemma on the structure of $\mathbf{G}_{\text{MMSE}}$ and $\mathbf{G}_{\text{ZF}}$.

Lemma 1. *For a 2×2 block matrix $\mathbf{H}_{MIMO}$ with blocks $\mathbf{H}_{ij} \in \mathcal{B}_{MN}, i, j \in \{1, 2\}$, the matrices $\mathbf{G}_{MMSE}$ and $\mathbf{G}_{ZF}$ are also 2×2 block matrices with blocks in $\mathcal{B}_{MN}$.*

Proof. We prove this for $\mathbf{G}_{\text{MMSE}}$. The proof for $\mathbf{G}_{\text{ZF}}$ also follows with similar steps. Consider $\mathbf{G}_{\text{MMSE}} = (\mathbf{H}_{\text{MIMO}}^H\mathbf{H}_{\text{MIMO}} + \sigma^2\mathbf{I})^{-1}\mathbf{H}^H$. Let $\mathbf{A} = (\mathbf{H}_{\text{MIMO}}^H\mathbf{H}_{\text{MIMO}} + \sigma^2\mathbf{I})$. Now, $\mathbf{A}$ can be written in the form

$$\mathbf{A} = \begin{bmatrix} \mathbf{A}_{11} & \mathbf{A}_{12} \\ \mathbf{A}_{21} & \mathbf{A}_{22} \end{bmatrix}, \tag{13}$$

$$\begin{aligned} \mathbf{A}_{11} =& \mathbf{H}_{11}^H\mathbf{H}_{11} + \mathbf{H}_{21}^H\mathbf{H}_{21} + \sigma^2\mathbf{I}, \;\; \mathbf{A}_{12} = \mathbf{H}_{11}^H\mathbf{H}_{12} + \mathbf{H}_{21}^H\mathbf{H}_{22}, \\ \mathbf{A}_{21} =& \mathbf{H}_{12}^H\mathbf{H}_{11} + \mathbf{H}_{22}^H\mathbf{H}_{21}, \;\; \mathbf{A}_{22} = \mathbf{H}_{12}^H\mathbf{H}_{12} + \mathbf{H}_{22}^H\mathbf{H}_{22} + \sigma^2\mathbf{I}. \end{aligned} \tag{14}$$

Here, observe that $\mathbf{H}_{ij} \in \mathcal{B}_{MN}$, $i, j \in \{1, 2\}$ and $\mathbf{A}_{ij}$s are composed of $\mathbf{H}_{ij}$s. Now, we use the following properties of $\mathcal{B}_{MN}$ to understand the structure of $\mathbf{A}_{ij}$s.

Property 1: For any matrix $\mathbf{P} \in \mathcal{B}_{MN}$, the matrices $\mathbf{P}^T$, $\mathbf{P}^H$, and $\mathbf{P}^{-1}$ (if exists) are all in $\mathcal{B}_{MN}$.

Property 2: For any two matrices $\mathbf{P}$, $\mathbf{Q} \in \mathcal{B}_{M,N}$, $\mathbf{PQ} \in \mathcal{B}_{MN}$, $\mathbf{QP} \in \mathcal{B}_{MN}$, and $\mathbf{PQ} = \mathbf{QP}$. Also, for any two scalars δ_1 and δ_2, $\delta_1\mathbf{P} + \delta_2\mathbf{Q} \in \mathcal{B}_{MN}$.

Now, using properties 1 and 2, it can be seen that the matrices $\mathbf{A}_{ij} \in \mathcal{B}_{MN}$, $i, j \in \{1, 2\}$. The inverse of the 2×2 block matrix $\mathbf{A}^{-1}$ is of the form given by

$$\mathbf{A}^{-1} = \begin{bmatrix} \mathbf{U}_{11} & \mathbf{U}_{12} \\ \mathbf{U}_{21} & \mathbf{U}_{22} \end{bmatrix}, \tag{15}$$

$$\begin{aligned} \mathbf{U}_{11} =& (\mathbf{A}_{11} - \mathbf{A}_{12}\mathbf{A}_{22}^{-1}\mathbf{A}_{21})^{-1}, \\ \mathbf{U}_{12} =& -\mathbf{A}_{11}^{-1}\mathbf{A}_{12}(\mathbf{A}_{22} - \mathbf{A}_{21}\mathbf{A}_{11}^{-1}\mathbf{A}_{12})^{-1}, \\ \mathbf{U}_{21} =& -\mathbf{A}_{22}^{-1}\mathbf{A}_{21}(\mathbf{A}_{11} - \mathbf{A}_{12}\mathbf{A}_{22}^{-1}\mathbf{A}_{21})^{-1}, \\ \mathbf{U}_{22} =& (\mathbf{A}_{22} - \mathbf{A}_{21}\mathbf{A}_{11}^{-1}\mathbf{A}_{12})^{-1}. \end{aligned} \tag{16}$$

Again, from properties 1 and 2, it can be seen that $\mathbf{U}_{ij} \in \mathcal{B}_{MN}$, $i, j \in \{1, 2\}$. Now, $\mathbf{G}_{\text{MMSE}} = \mathbf{A}^{-1}\mathbf{H}_{\text{MIMO}}^H$ is given by

$$\mathbf{G}_{\text{MMSE}} = \begin{bmatrix} \mathbf{U}_{11} & \mathbf{U}_{12} \\ \mathbf{U}_{21} & \mathbf{U}_{22} \end{bmatrix} \begin{bmatrix} \mathbf{H}_{11}^* & \mathbf{H}_{21}^* \\ \mathbf{H}_{12}^* & \mathbf{H}_{22}^* \end{bmatrix} = \begin{bmatrix} \mathbf{G}_{11} & \mathbf{G}_{12} \\ \mathbf{G}_{21} & \mathbf{G}_{22} \end{bmatrix}, \tag{17}$$

$$\begin{aligned} \mathbf{G}_{11} =& \mathbf{U}_{11}\mathbf{H}_{11}^* + \mathbf{U}_{12}\mathbf{H}_{12}^*, \mathbf{G}_{12} = \mathbf{U}_{11}\mathbf{H}_{21}^* + \mathbf{U}_{12}\mathbf{H}_{22}^*, \\ \mathbf{G}_{21} =& \mathbf{U}_{21}\mathbf{H}_{11}^* + \mathbf{U}_{22}\mathbf{H}_{12}^*, \mathbf{G}_{22} = \mathbf{U}_{21}\mathbf{H}_{21}^* + \mathbf{U}_{22}\mathbf{H}_{22}^*. \end{aligned} \tag{18}$$

Again, from properties 1 and 2 it can be seen that $\mathbf{G}_{ij} \in \mathcal{B}_{MN}$, $i, j \in \mathcal{B}_{MN}$. Therefore, $\mathbf{G}_{\text{MMSE}}$ is a block matrix such that $\mathbf{G}_{ij} \in \mathcal{B}_{MN}$. □

Since $\mathbf{G}_{ij} \in \mathcal{B}_{MN}, i, j \in \{1, 2\}$, the EVD of $\mathbf{G}_{ij}$ is of the form

$$\mathbf{G}_{ij} = (\mathbf{F}_M \otimes \mathbf{F}_N)^H\mathbf{\Gamma}_{ij}(\mathbf{F}_M \otimes \mathbf{F}_N), \tag{19}$$

where $\mathbf{\Gamma}_{ij}$ denotes $MN \times MN$ diagonal matrix containing the eigen values of $\mathbf{G}_{ij}$. Therefore, $\mathbf{G}_{\text{MMSE}}$ can be written as

$$\mathbf{G}_{\text{MMSE}} = (\mathbf{I}_{n_t} \otimes (\mathbf{F}_M \otimes \mathbf{F}_N)^H)\mathbf{\Gamma}_{\text{eff}}(\mathbf{I}_{n_t} \otimes (\mathbf{F}_M \otimes \mathbf{F}_N)), \tag{20}$$

where $\mathbf{\Gamma}_{\text{eff}}$ is given by

$$\mathbf{\Gamma}_{\text{eff}} = \begin{bmatrix} \mathbf{\Gamma}_{11} & \mathbf{\Gamma}_{12} \\ \mathbf{\Gamma}_{21} & \mathbf{\Gamma}_{22} \end{bmatrix}. \tag{21}$$

Therefore, the MMSE solution is of the form

$$\hat{\mathbf{x}}_{\text{MMSE}} = (\mathbf{I}_{n_t} \otimes (\mathbf{F}_M \otimes \mathbf{F}_N)^H)\mathbf{\Gamma}_{\text{eff}}(\mathbf{I}_{n_t} \otimes (\mathbf{F}_M \otimes \mathbf{F}_N))\mathbf{y}_{\text{MIMO}}. \tag{22}$$

It can be observed that the computation of $\hat{\mathbf{x}}_{\text{MMSE}}$ in (22) requires the computation of $\mathbf{\Gamma}_{\text{eff}}$, which, in turn, involves the computation of $\mathbf{\Gamma}_{ij}$ for $i, j \in \{1, 2\}$.

Computation of $\mathbf{\Gamma}_{ij}s$: In order to compute $\mathbf{\Gamma}_{ij}$s, we follow the following approach. We first compute the eigen values of the effective delay-Doppler MIMO channel matrix $\mathbf{H}_{\text{MIMO}}$ using (12). We then compute $\mathbf{\Gamma}_{ij}$s by expressing $\mathbf{\Gamma}_{ij}s$ in terms of $\mathbf{\Lambda}_{ij}$s. Computing $\mathbf{\Gamma}_{ij}$s from $\mathbf{\Lambda}_{ij}$s constitutes one of the important steps in the proposed algorithm. Consider the 2×2 block matrix $\mathbf{A}$ in (13). The blocks $\mathbf{A}_{ij} \in \mathcal{B}_{MN}, i, j \in \{1, 2\}$, and hence the EVD of $\mathbf{A}_{ij}$ is of the form

$$\mathbf{A}_{ij} = (\mathbf{F}_M \otimes \mathbf{F}_N)^H\mathbf{\Phi}_{ij}(\mathbf{F}_M \otimes \mathbf{F}_N), \tag{23}$$

where $\mathbf{\Phi}_{ij}$ is $NM \times NM$ diagonal matrix which contains the eigen values of $\mathbf{A}_{ij}$. Now, substituting (11) in (14) and comparing it with (23), $\mathbf{\Phi}_{ij}$s can be expressed in terms of $\mathbf{\Lambda}_{ij}$s as

$$\begin{aligned} \mathbf{\Phi}_{11} =& \mathbf{\Lambda}_{11}^H\mathbf{\Lambda}_{11} + \mathbf{\Lambda}_{21}^H\mathbf{\Lambda}_{21} + \sigma^2\mathbf{I}, \;\; \mathbf{\Phi}_{12} = \mathbf{\Lambda}_{11}^H\mathbf{\Lambda}_{12} + \mathbf{\Lambda}_{21}^H\mathbf{\Lambda}_{22}, \\ \mathbf{\Phi}_{21} =& \mathbf{\Lambda}_{12}^H\mathbf{\Lambda}_{11} + \mathbf{\Lambda}_{22}^H\mathbf{\Lambda}_{21}, \;\; \mathbf{\Phi}_{22} = \mathbf{\Lambda}_{12}^H\mathbf{\Lambda}_{12} + \mathbf{\Lambda}_{22}^H\mathbf{\Lambda}_{22} + \sigma^2\mathbf{I}. \end{aligned} \tag{24}$$

Next, consider $\mathbf{A}^{-1}$, which is also a block matrix with blocks $\mathbf{U}_{ij} \in \mathcal{B}_{MN}, i, j \in \{1, 2\}$. The EVD of $\mathbf{U}_{ij}$ is given by

$$\mathbf{U}_{ij} = (\mathbf{F}_M \otimes \mathbf{F}_N)^H\mathbf{\Psi}_{ij}(\mathbf{F}_M \otimes \mathbf{F}_N), \tag{25}$$

where $\mathbf{\Psi}_{ij}$ denotes $NM \times NM$ diagonal matrix which contains the eigen values of $\mathbf{U}_{ij}$. Substituting (23) in (16) and comparing it with (25), $\mathbf{\Psi}_{ij}$s can be expressed in terms of $\mathbf{\Phi}_{ij}$s as

$$\begin{aligned} \mathbf{\Psi}_{11} =& (\mathbf{\Phi}_{11} - \mathbf{\Phi}_{12}\mathbf{\Phi}_{22}^{-1}\mathbf{\Phi}_{21})^{-1}, \\ \mathbf{\Psi}_{12} =& -\mathbf{\Phi}_{11}^{-1}\mathbf{\Phi}_{12}(\mathbf{\Phi}_{22} - \mathbf{\Phi}_{21}\mathbf{\Phi}_{11}^{-1}\mathbf{\Phi}_{12})^{-1}, \\ \mathbf{\Psi}_{21} =& \mathbf{\Phi}_{22}^{-1}\mathbf{\Phi}_{21}(\mathbf{\Phi}_{11} - \mathbf{\Phi}_{12}\mathbf{\Phi}_{22}^{-1}\mathbf{\Phi}_{21})^{-1}, \\ \mathbf{\Psi}_{22} =& (\mathbf{\Phi}_{22} - \mathbf{\Phi}_{21}\mathbf{\Phi}_{11}^{-1}\mathbf{\Phi}_{12})^{-1}. \end{aligned} \tag{26}$$

Finally, observe that $\mathbf{G} = \mathbf{A}^{-1}\mathbf{H}^H$ is also a 2×2 block matrix with blocks $\mathbf{G}_{ij} \in \mathcal{B}_{MN}$. The EVD of $\mathbf{G}_{ij}$ is given by (19). Now, substituting (25) and (11) in (18) and comparing it with (19), $\mathbf{\Gamma}_{ij}$ can be expressed in terms of $\mathbf{\Psi}_{ij}$ and $\mathbf{\Lambda}_{ij}$ as

$$\begin{aligned} \mathbf{\Gamma}_{11} =& \mathbf{\Psi}_{11}\mathbf{\Lambda}_{11}^* + \mathbf{\Psi}_{12}\mathbf{\Lambda}_{12}^*, \;\; \mathbf{\Gamma}_{12} = \mathbf{\Psi}_{11}\mathbf{\Lambda}_{21}^* + \mathbf{\Psi}_{12}\mathbf{\Lambda}_{22}^*, \\ \mathbf{\Gamma}_{21} =& \mathbf{\Psi}_{21}\mathbf{\Lambda}_{11}^* + \mathbf{\Psi}_{22}\mathbf{\Lambda}_{12}^*, \;\; \mathbf{\Gamma}_{22} = \mathbf{\Psi}_{21}\mathbf{\Lambda}_{21}^* + \mathbf{\Psi}_{22}\mathbf{\Lambda}_{22}^*. \end{aligned} \tag{27}$$

Observe that since $\mathbf{\Psi}_{ij}$s can be expressed in terms of $\mathbf{\Phi}_{ij}$s, which, in turn, can be expressed in terms of $\mathbf{\Lambda}_{ij}$s, $\mathbf{\Gamma}_{ij}$s in (27) can be computed from $\mathbf{\Lambda}_{ij}$s. The computation of $\mathbf{\Gamma}_{ij}$s from $\mathbf{\Lambda}_{ij}$s can be done by substituting (26) and (24) in (27). Therefore, the eigen values of $\mathbf{G}_{\text{MMSE}}$ can be obtained from the eigen values of $\mathbf{H}_{\text{MIMO}}$. This is one of the main ideas in the proposed low-complexity equalizer for 2×2 MIMO-OTFS system. We now describe the steps involved in the implementation of low-complexity MMSE equalizer.

1) *Step 1: Computation of eigen values of $\mathbf{H}_{ij}s$:* The first step in the proposed MMSE equalizer involves computing eigen values of each block of $\mathbf{H}_{\text{MIMO}}$ (i.e., $\mathbf{H}_{ij}, i, j \in$

$\{1,2\}\big)$. The eigen values of $\mathbf{H}_{ij}$ are given using (12), which can be written as

$$\mathbf{\Lambda}_{ij} = \text{diag}\Big\{ \textstyle\sum_{k=0}^{M-1} \mathbf{\Lambda}_{ij}^{(k)},\ \sum_{k=0}^{M-1} e^{j2\pi k/M}\mathbf{\Lambda}_{ij}^{(k)},\ \cdots,\ \sum_{k=0}^{M-1} e^{j2\pi(M-1)k/M}\mathbf{\Lambda}_{ij}^{(k)} \Big\}. \quad (28)$$

Here, $\mathbf{\Lambda}_{ij}^{(k)}$ denotes $N\times N$ diagonal matrix which contains the eigen values of kth circulant block of $\mathbf{H}_{ij}$. The diagonal matrices $\mathbf{\Lambda}_{ij}^{(k)}$s containing the eigen values of the circulant blocks of $\mathbf{H}_{ij}$ are obtained by computing the DFTs of first row of each block of $\mathbf{H}_{ij}$. Therefore, for a given $\mathbf{H}_{ij}$, the computation of $\mathbf{\Lambda}_{ij}^{(k)}$ for $k = 0, 1, \cdots, M-1$ involves computation of M N-point DFTs, requiring a complexity of $\mathcal{O}(MN\log N)$. Further, $\mathbf{\Lambda}_{ij}^{(k)}$s are used to compute $\mathbf{\Lambda}_{ij}$s in (28). Now, observe that (28) can be computed as $\text{diag}(\mathbf{F}_M^H\mathbf{C}_{ij})^T$, where $\mathbf{C}_{ij}$ is $M\times N$ matrix whose rth row contains diagonal elements of $\mathbf{\Lambda}_{ij}^{(r)}$. Therefore, $\mathbf{\Lambda}_{ij}$ in (28) can be written as

$$\mathbf{\Lambda}_{ij} = \text{diag}\{(\mathbf{F}_M^H\mathbf{C}_{ij})^T\}. \quad (29)$$

The complexity of computing (29) is $\mathcal{O}(MN\log M)$. Therefore, the total complexity involved in computing $\mathbf{\Lambda}_{ij}$ $i,j\in\{1,2\}$ is $\mathcal{O}(MN\log MN)$.

2) *Step 2: Computation of eigen values of $\mathbf{G}_{MMSE}$ using eigen values $\mathbf{H}_{ij}$s:* Next, the eigen values of $\mathbf{G}_{\text{MMSE}}$ (i.e., $\mathbf{\Gamma}_{ij}$s) are computed using the eigen values of $\mathbf{H}_{ij}$s (i.e., $\mathbf{\Lambda}_{ij}$s) using (24), (26), and (27). Since the matrices involved in (24), (26), and (27) (i.e., $\mathbf{\Lambda}_{ij}$, $\mathbf{\Phi}_{ij}$, $\mathbf{\Psi}_{ij}$) are all diagonal matrices, the order of complexity involved in computing $\mathbf{\Gamma}_{ij}$s from $\mathbf{\Lambda}_{ij}$s is $\mathcal{O}(MN)$.

3) *Step 3: Computation of $\mathbf{G}_{MMSE}\mathbf{y}_{MIMO}$:* Here, we compute $\mathbf{G}_{\text{MMSE}}\mathbf{y}_{\text{MIMO}} = (\mathbf{I}_{n_t}\otimes(\mathbf{F}_M\otimes\mathbf{F}_N)^H)\mathbf{\Gamma}_{\text{eff}}(\mathbf{I}_{n_t}\otimes(\mathbf{F}_M\otimes\mathbf{F}_N))\mathbf{y}_{\text{MIMO}}$, which can be carried out at a reduced complexity using FFTs and IFFTs. Let $\tilde{\mathbf{Y}}$ denote $MN\times 2$ matrix with kth column being $NM\times 1$ vector received at kth antenna. Therefore, $\tilde{\mathbf{Y}} = [\mathbf{y}_1\ \ \mathbf{y}_2]$, where $\mathbf{y}_1$ and $\mathbf{y}_2$ denote $NM\times 1$ vectors received at the first and second antennas, respectively. Now, $(\mathbf{I}_{n_t}\otimes(\mathbf{F}_M\otimes\mathbf{F}_N))\mathbf{y}_{\text{MIMO}}$ can be written as

$$\mathbf{q} = (\mathbf{I}_{n_t}\otimes(\mathbf{F}_M\otimes\mathbf{F}_N))\mathbf{y}_{\text{MIMO}} = \text{vec}\{(\mathbf{F}_M\otimes\mathbf{F}_N)\tilde{\mathbf{Y}}\}. \quad (30)$$

Further, let $\mathbf{Y}_1$ and $\mathbf{Y}_2$ denote $N\times M$ matrices such that $\mathbf{Y}_1 = \text{vec}(\mathbf{y}_1)$ and $\mathbf{Y}_2 = \text{vec}(\mathbf{y}_2)$. Now,

$$\mathbf{q} = \text{vec}[\text{vec}(\mathbf{F}_N\mathbf{Y}_1\mathbf{F}_M^H)\ \ \text{vec}(\mathbf{F}_N\mathbf{Y}_1\mathbf{F}_M^H)]. \quad (31)$$

Observe that the computation of $(\mathbf{F}_N\mathbf{Y}_1\mathbf{F}_M^H)$ involves the computation of N-point FFT along the columns of $\mathbf{Y}_1$ and M-point IFFT along the rows of $\mathbf{Y}_1$. Therefore, computing $(\mathbf{F}_N\mathbf{Y}_1\mathbf{F}_M^H)$ involves a complexity of $\mathcal{O}(MN\log MN)$ and hence computing $\mathbf{q}$ involves a complexity of $\mathcal{O}(MN\log MN)$. Next, $\mathbf{r} = \mathbf{\Gamma}_{\text{eff}}\mathbf{q}$ is computed. Since $\mathbf{\Gamma}_{ij}$s are all $MN\times MN$ diagonal matrices, the computation of $\mathbf{\Gamma}_{\text{eff}}\mathbf{q}$ requires a complexity of $\mathcal{O}(MN)$. Finally, the computation of $\mathbf{G}_{\text{MMSE}}\mathbf{y}_{\text{MIMO}} = (\mathbf{I}_{n_t}\otimes(\mathbf{F}_M\otimes\mathbf{F}_N)^H)\mathbf{r}$ is performed similar to the computation of $\mathbf{q}$. Let $\mathbf{r}_1$ denote the $NM\times 1$ vector containing the first NM entries of $\mathbf{r}$, $\mathbf{r}_2$ denote the $NM\times 1$ vector containing the next NM entries of $\mathbf{r}$, and let $\tilde{\mathbf{R}}$ denote $NM\times 2$ matrix s.t. $\text{vec}(\tilde{\mathbf{R}}) = \mathbf{r}$. Now,

$$\begin{aligned}\mathbf{G}_{\text{MMSE}}\mathbf{y}_{\text{MIMO}} &= \text{vec}\{(\mathbf{F}_M\otimes\mathbf{F}_N)\tilde{\mathbf{R}}\}\\ &= \text{vec}[\text{vec}(\mathbf{F}_N\mathbf{R}_1\mathbf{F}_M^H)\ \ \text{vec}(\mathbf{F}_N\mathbf{R}_1\mathbf{F}_M^H)],\end{aligned} \quad (32)$$

where $\mathbf{R}_1 = \text{vec}(\mathbf{r}_1)$ and $\mathbf{R}_2 = \text{vec}(\mathbf{r}_2)$. Similar to the computation of $\mathbf{q}$, the computation of (32) involves a complexity of $\mathcal{O}(MN\log MN)$. Therefore, the overall complexity involved in the computation of $\mathbf{G}_{\text{MMSE}}\mathbf{y}_{\text{MIMO}}$ in step 3 is $\mathcal{O}(MN\log MN)$.

B. Low complexity ZF equalizer

The ZF solution is given by $\mathbf{G}_{\text{ZF}}\mathbf{y}_{\text{MIMO}}$, where $\mathbf{G}_{\text{ZF}} = (\mathbf{H}_{\text{MIMO}}^H\mathbf{H}_{\text{MIMO}})^{-1}\mathbf{H}_{\text{MIMO}}^H$. Similar to $\mathbf{G}_{\text{MMSE}}$, the matrix $\mathbf{G}_{\text{ZF}}\in\mathcal{B}_{MN}$. Hence, $\mathbf{G}_{\text{ZF}}$ can be written in the form

$$\mathbf{G}_{\text{ZF}} = (\mathbf{I}_{n_t}\otimes(\mathbf{F}_M\otimes\mathbf{F}_N)^H)\mathbf{\Upsilon}_{\text{eff}}(\mathbf{I}_{n_t}\otimes(\mathbf{F}_M\otimes\mathbf{F}_N)), \quad (33)$$

where

$$\mathbf{\Upsilon}_{\text{eff}} = \begin{bmatrix}\mathbf{\Upsilon}_{11} & \mathbf{\Upsilon}_{12}\\ \mathbf{\Upsilon}_{21} & \mathbf{\Upsilon}_{22}\end{bmatrix}, \quad (34)$$

and $\mathbf{\Upsilon}_{ij}\in\mathcal{B}_{MN}$. The computation of $\mathbf{\Upsilon}_{ij}$s from $\mathbf{\Lambda}_{ij}$s is similar to computing $\mathbf{\Gamma}_{ij}$s from $\mathbf{\Lambda}_{ij}$ as discussed in Sec. III-A. As in the case of the low-complexity MMSE equalizer, the complexity of the above low-complexity ZF equalizer is $\mathcal{O}(MN\log MN)$. The complexity orders associated with various steps of the proposed equalizers are given in Table I.

TABLE I: Complexity of proposed low-complexity equalizers

Step #	**Order of complexity**
1: Computation of eigen values of $\mathbf{H}_{ij}$, $i,j\in\{1,2\}$	$\mathcal{O}(MN\log MN)$
2: Computation of $\mathbf{\Gamma}_{\text{eff}}$ / $\mathbf{\Upsilon}_{\text{eff}}$ from $\mathbf{\Lambda}_{ij}$s	$\mathcal{O}(MN)$
3: Computation of $\mathbf{G}_{\text{MMSE}}\mathbf{y}_{\text{MIMO}}$/ $\mathbf{G}_{\text{ZF}}\mathbf{y}_{\text{MIMO}}$	$\mathcal{O}(MN\log MN)$
Overall complexity (dominated by **Step 3**)	$\mathcal{O}(MN\log MN)$

Remark: The derivation of the proposed equalizer makes use of the expression for inverse of a 2×2 block matrix and the properties of block circulant with circulant block structure of each block. Extension of the proposed equalizer for a general $n_r\times n_t$ MIMO-OTFS system requires simplifying the inverse of a larger matrix. Although the inverse of an $n_r\times n_t$ block matrix can be computed by viewing it as a 2×2 block matrix with larger blocks, each block in this case will not have a block circulant with circulant block structure as in the case of 2×2 MIMO-OTFS. Hence, this extension is not considered in the present work and is a potential topic for future work.

IV. Results and Discussions

Figure 1 shows the bit error rate (BER) performance of 2×2 MIMO-OTFS with conventional and the proposed MMSE and ZF equalizers. We consider a MIMO-OTFS system with $n_t = n_r = 2$, $M = 64$, $N = 12$. A carrier frequency of 4 GHz, subcarrier spacing of 15 kHz, and BPSK modulation are considered. A channel with $P = 8$ paths with exponential power delay profile and Jakes' Doppler spectrum is considered for the simulations. The considered delay profile is $\{\tau_i, i = 0,\cdots,P-1\} =$

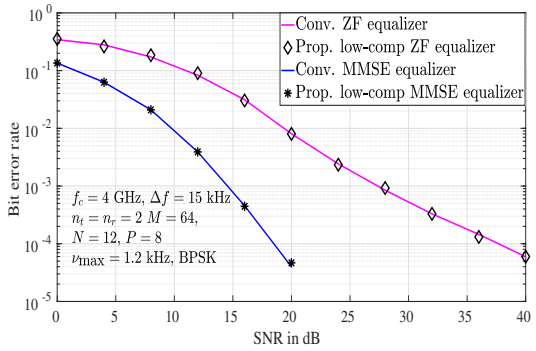

Fig. 1: BER performance of the proposed low-complexity MMSE and ZF equalizers for 2×2 MIMO-OTFS system.

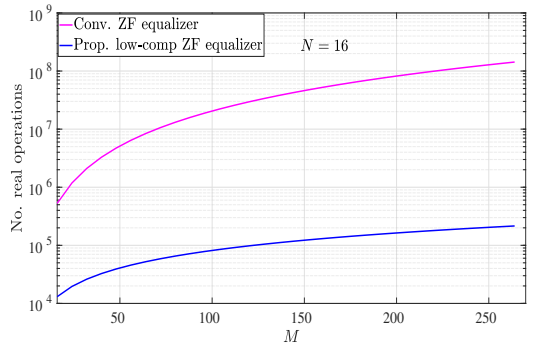

Fig. 2: Complexity (in number of real operations) of the proposed ZF equalizer as a function of M.

$\{0, 1.04, 2.08, 3.12, 4.16, 5.20, 6.25, 7.29\}$ μs and the Doppler shifts ν_is associated with each path are generated according to $\nu_i = \nu_{\max} \cos\theta_i$, where $\nu_{\max}$ is the maximum Doppler shift in the channel and θ_is are distributed uniformly over $[-\pi\ \pi]$. A maximum Doppler shift of 1.2 kHz is considered for the simulations. From Fig. 1, we observe that the performance of 2×2 MIMO-OTFS with MMSE equalizer is superior to that of ZF equalizer. Further, the BER with the proposed reduced complexity MMSE and ZF equalizers overlap with that of the conventional MMSE and ZF equalizers, respectively, demonstrating that the proposed equalizers provide exactly same solutions as those of the conventional equalizers.

Figure 2 shows a comparison of computational complexity of the proposed low-complexity ZF equalizer with that of the conventional ZF equalizer. We consider a 2×2 MIMO-OTFS system with $N = 16$ and plot the computational complexity in terms of the number of real operations as a function M. All other parameters are same as those used in Fig. 1. From Fig. 2, we observe that the the proposed low-complexity ZF equalizer has significantly lower complexity compared to that of conventional ZF equalizer. For example, the number of real operations required to obtain ZF solution for $M = 256$ and $N = 16$ is 215437 in case of proposed low-complexity ZF equalizer, whereas the conventional equalizer requires a complexity of 1.4×10^8 real operations.

Figure 3 shows the comparison of computational complexity of proposed MMSE equalizer with that of the conventional MMSE equalizer, as a function of M. The simulation uses $N = 16$ and all other parameters used are same as those used in Fig 1. From Fig. 3, we observe that the proposed MMSE equalizer has significantly lower complexity compared to that of the conventional MMSE equalizer. For example, for $M = 256$, $N = 16$, the complexity of the proposed MMSE equalizer is 333711 operations, whereas the complexity of the conventional equalizer is 2.19×10^{12}.

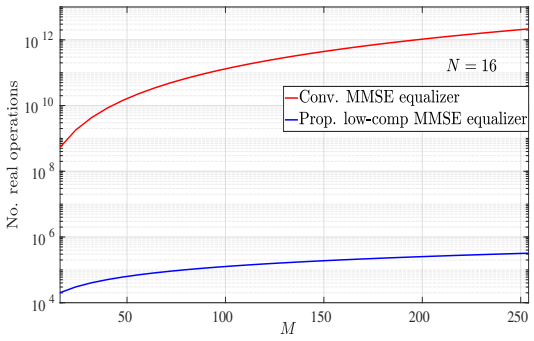

Fig. 3: Complexity (in number of real operations) of the proposed MMSE equalizer as a function of M.

V. Conclusions

We proposed low-complexity linear equalizers for a 2×2 MIMO-OTFS system. We derived exact ZF and MMSE equalizers of low complexities by exploiting the structure of the effective delay-Doppler MIMO channel matrix in a 2×2 MIMO-OTFS system. We demonstrated that the proposed low-complexity equalizers provide exact solutions at significantly reduced complexities compared to those of conventional linear equalizers. Obtaining exact solutions at low complexities can lead to efficient realizations of non-linear equalizers which rely on MMSE/ZF equalizers for initial solutions.

References

[1] A. Monk, R. Hadani, M. Tsatsanis, and S. Rakib, "OTFS - orthogonal time frequency space: a novel modulation technique meeting 5G high mobility and massive MIMO challenges," online: arXiv:1608.02993 [cs.IT] 9 Aug 2016.

[2] R. Hadani, S. Rakib, M. Tsatsanis, A. Monk, A. J. Goldsmith, A. F. Molisch, and R. Calderbank, "Orthogonal time frequency space modulation," *Proc. IEEE WCNC'2017*, pp. 1-7, Mar. 2017.

[3] R. Hadani, S. Rakib, S. Kons, M. Tsatsanis, A. Monk, C. Ibars, J. Delfeld, Y. Hebron, A. J. Goldsmith, A. F. Molisch, and R. Calderbank, "Orthogonal time frequency space modulation," online: arXiv:1808.00519v1 [cs.IT] 1 Aug 2018.

[4] P. Raviteja, K. T. Phan, Y. Hong, and E. Viterbo, "Interference cancellation and iterative detection for orthogonal time frequency space modulation," *IEEE Trans. Wireless Commun.*, vol. 17, no. 10, pp. 6501-6515, Aug. 2018.

[5] K. R. Murali and A. Chockalingam, "On OTFS modulation for high-Doppler fading channels," *Proc. ITA'2018*, San Diego, Feb. 2018.

[6] A. Nimr, M. Chafii, M. Matthe, and G. Fettweis, "Extended GFDM framework: OTFS and GFDM comparison," *Proc. IEEE GLOBECOM'2018*, Dec. 2018.

[7] T. Zemen, M. Hofer, and D. Loeschenbrand, "Low-complexity equalization for orthogonal time and frequency signaling (OTFS)," Online: arXiv:1710.09916v1 [cs.IT] 26 Oct 2017.

[8] S. Tiwari, S. S. Das, and V. Rangamgari, "Low complexity LMMSE receiver for OTFS," *IEEE Commun. Lett.*, vol. 23, no. 12, pp. 2205-2209, Dec. 2019.

[9] G. D. Surabhi and A. Chockalingam, "Low-complexity linear equalization for OTFS modulation," *IEEE Commun. Lett.*, vol. 24, no. 2, pp. 330-334, Feb. 2020.

[10] M. K. Ramachandran and A. Chockalingam, "MIMO-OTFS in high-Doppler fading channels: signal detection and channel estimation," *Proc. IEEE GLOBECOM'2018*, Dec. 2018.

[11] P. J. Davis, *Circulant Matrices*, American Mathematical Society, 2012.